Journal of Magnetic Resonance **140,** 58–68 (1999)
Article ID jmre.1999.1830, available online at http://www.idealibrary.com on IDEAL®

An Optimized Pulse Sequence for Isotropically Weighted Diffusion Imaging

M. Cercignani[1] and M. A. Horsfield

Division of Medical Physics, University of Leicester, Leicester Royal Infirmary, Leicester LE1 5WW, United Kingdom

Received September 25, 1998; revised April 27, 1999

Single-shot echo-planar imaging is becoming the most widely used technique for magnetic resonance diffusion imaging, since it enables measurement of diffusion coefficients in human brain without motion artifacts. However, its reliability is limited by geometrical distortions due to eddy currents. In this report, an isotropically weighted echo-planar pulse sequence, optimized to give the maximum signal-to-noise ratio in the computed trace image and designed to produce inherently low distortions, is presented. It is also shown how the residual translational distortion can be easily characterized and removed by postprocessing. A full characterization of the distortion artifact involves a few measurements on a phantom, in order to estimate the distortion as a function of slice orientation, which can then be used to correct any slice orientation. Results of applying the image translation correction to data collected from a patient are presented.

Key Words: **diffusion-weighted imaging; echo planar; isotropic weighting; distortion correction; eddy currents.**

INTRODUCTION

Variations in the measured self-diffusion coefficient of tissue water accompany physiological differences in tissue at the microscopic level. MRI measures of diffusion have so far proved to be useful in the diagnosis of abnormalities, particularly with regard to stroke (*1–5*), but the technique also has a great deal of potential in other diseases such as tumors (*6*) and in demyelinating disorders (*7, 8*). Conventional spin-echo diffusion-weighted (DW) images are, however, highly sensitive to motion artifacts, such as cardiac-cycle-related pulsations, involuntary subject movement, and flow of the cerebrospinal fluid, due to the large gradients applied (*9*). Single-shot echo-planar imaging (EPI), on the other hand, enables robust DW imaging without significant motion artifacts, since all the lines of *k* space are filled in a single acquisition, and thus no phase discontinuity arises between successive lines (*10*). The implementation of echo-planar DW MRI on commercial scanners has resulted in a much more widespread dissemination of the technique into the radiological community.

Since DW images are also inevitably T_2-weighted, the radiological interpretation of DW images is not without difficulty. For this reason, it is desirable to produce a calculated image of the apparent diffusion coefficient (ADC) from a combination of an image without diffusion weighting and an image with weighting; this requires that the two images be correctly registered. Unfortunately, diffusion weighting of echo-planar images usually results in significant eddy currents induced by the strong gradient pulses applied in DW imaging. Because of the low bandwidth in the phase-encoded direction of echo-planar images, the eddy currents give rise to geometric distortions in the phase-encode direction: a shift, shear, and stretch on the image (*11*).

Furthermore, diffusion anisotropy, while being a potentially useful source of information about tissue structure, may also result in difficulties when interpreting changes in the diffusion constant. With diffusion weighting applied in a single direction, a bright region on a DW image may be due either to a focal abnormality or to the particular alignment of tissue structures. It is, therefore, a good idea to use pulse sequences that give contrast depending on the trace of the diffusion tensor, a rotationally invariant measure of average diffusivity (*12, 13*).

There are several ways of achieving rotationally invariant measures: the simplest is to separately apply the diffusion gradients in three orthogonal directions to produce three DW images. The ADC maps for the three directions are then calculated and averaged (*13*), and of course this solution requires at least four images, including the unweighted image. Alternatively, diffusion-sensitizing gradient schemes that result in isotropic weighting can be used. Some very efficient schemes have been designed to give attenuation due to the trace of the diffusion tensor, and have diffusion-encoding gradients applied on three axes (*14, 15*). When used in conjunction with single-shot EPI, this allows the collection of images without motion artifacts, where the intensity is independent of tissue cell orientation.

In this report, we show that isotropically weighted sequences can be designed to have inherently low geometrical distortions due to gradient eddy currents. We characterize most of the

[1] Permanent address: Neuroimaging Research Unit, Department of Neurology, Scientific Institute Ospedale San Raffaele, University of Milan, Via Olgettina, 60, Milan 20132, Italy.

1090-7807/99 $30.00

remaining geometrical distortions occurring with an isotropically weighted sequence and suggest a simple processing scheme to remove them. The characterization of the distortion can be performed using a phantom, and the correction can then be applied retrospectively on patient data.

THEORY

General

The signal attenuation equation occurring in a spin-echo sequence, with echo time TE, due to transverse relaxation and anisotropic diffusion is given by (*12*)

$$S = S_0 \exp\left(-\frac{\mathrm{TE}}{T_2}\right) \exp\left(-\sum_{i=1}^{3}\sum_{j=1}^{3} b_{i,j} D_{i,j}\right). \qquad [1]$$

S_0 is the signal intensity without diffusion weighting and relaxation; **b** is the gradient *b*-factor matrix; and **D** is the 3×3 symmetric diffusion tensor matrix. **D** is of the form

$$\mathbf{D} = \begin{bmatrix} D_{xx} & D_{xy} & D_{xz} \\ D_{xy} & D_{yy} & D_{yz} \\ D_{xz} & D_{yz} & D_{zz} \end{bmatrix}, \qquad [2]$$

and the elements of **b** are calculated from

$$b_{i,j} = \gamma^2 \int_0^{\mathrm{TE}} k_i(t') k_j(t') dt', \quad i, j \in [x, y, z], \qquad [3]$$

where $\mathbf{k}(t')$ is the *k*-space trajectory vector. **b** accounts for interactions both between imaging and diffusion gradients applied in the same direction (diagonal terms) and in perpendicular directions (off-diagonal terms). For isotropic diffusion, the off-diagonal elements of the **D** matrix are all zero, and the on-diagonal terms are all the same.

Often it is desirable to remove the effect of tissue alignment, and thus measure a quantity which is invariant with respect to rotations of the coordinate system or independent of tissue fiber direction. One of these quantities is the trace of the tensor,

$$\mathrm{Tr}(\mathbf{D}) = D_{xx} + D_{yy} + D_{zz}, \qquad [4]$$

which is a function only of the eigenvalues of **D** (*12*), and consequently it is a measure of the intrinsic properties of the medium.

Isotropically Weighted Gradient Design

Isotropically weighted imaging sequences aim to produce an image which has contrast dependent only on the trace of the diffusion tensor (and T_2 weighting). As can be seen from Eqs. [1] and [4], in order to achieve this, it is necessary to remove any effect of the off-diagonal terms of the tensor matrix. This can be achieved by imposing the following condition on the *k*-space trajectory (*14*):

$$\int_0^{\mathrm{TE}} k_x(t') k_y(t') dt' = \int_0^{\mathrm{TE}} k_x(t') k_z(t') dt' = \int_0^{\mathrm{TE}} k_y(t') k_z(t') dt' = 0. \qquad [5]$$

If, in addition, the following condition is satisfied,

$$\int_0^{\mathrm{TE}} (k_x(t'))^2 dt' = \int_0^{\mathrm{TE}} (k_y(t'))^2 dt' = \int_0^{\mathrm{TE}} (k_z(t'))^2 dt', \qquad [6]$$

then the on-diagonal elements of the **b** matrix are all equal:

$$b_{xx} = b_{yy} = b_{zz} = b. \qquad [7]$$

The signal attenuation can then be related directly to the trace of the diffusion tensor:

$$\frac{S}{S_0} = \exp\left(-\frac{\mathrm{TE}}{T_2}\right) \exp[-b(D_{xx} + D_{yy} + D_{zz})]. \qquad [8]$$

Optimization of Diffusion Weighting

According to Eq. [8], which describes signal attenuation, at least two images are needed to estimate Tr(**D**), performed with two different *b* values, while maintaining the same TE.

If transverse relaxation is ignored, it was shown by Bito *et al.* (*16*) that for isotropic diffusion, if an estimate of the diffusion coefficient, *D*, is to be made from two measurements, then the first should be done with the minimum possible weighting (b_1), and the second diffusion weighting (b_2) is such that

$$(b_2 - b_1) D = 1.109. \qquad [9]$$

If time permits, the signal-to-noise ratio in the calculated trace image can be improved by increasing the number of images acquired. However, just two *b* factors should still be used, with multiple measurements for each *b* factor. In the limit of a very large number of measurements, the number of measurements at the high *b* factor (N_{H}) should be 3.6 times the number at the low *b* factor (N_{L}), and the optimal difference in the *b* factors is $1.28/D$.

For a sequence that is weighted by the trace of the diffusion tensor, as described in the section above, following the same

reasoning as Bito, we now minimize the standard deviation of the estimated trace,

$$\sigma_{\mathrm{Tr}} = \left[\left(\frac{\partial\ \mathrm{Tr}(\mathbf{D})}{\partial S_0} \right)^2 \frac{\sigma^2}{N_{\mathrm{L}}} + \left(\frac{\partial\ \mathrm{Tr}(\mathbf{D})}{\partial S_1} \right)^2 \frac{\sigma^2}{(N - N_{\mathrm{L}})} \right]^{1/2}, \quad [10]$$

where N is the total number of measurements, equal to $N_{\mathrm{H}} + N_{\mathrm{L}}$. When a large number of measurements can be made, the optimal ratio of N_{H} to N_{L} can be calculated differentiating σ_{Tr} with respect to both b_{xx} and N_{L}:

$$\frac{\partial \sigma_{\mathrm{Tr}}}{\partial b_{xx}} = \frac{\sigma^2[\mathrm{Tr}(\mathbf{D}) b_{xx} N_{\mathrm{L}} \exp\{2 b_{xx} \mathrm{Tr}(\mathbf{D})\} - N + N_{\mathrm{L}} - \exp\{2 b_{xx} \mathrm{Tr}(\mathbf{D})\} N_{\mathrm{L}}]}{\left[\frac{\sigma^2 (N - N_{\mathrm{L}} + \exp\{2 b_{xx} \mathrm{Tr}(\mathbf{D})\} N_{\mathrm{L}})}{S_0^2 {b_{xx}}^2 N_{\mathrm{L}} (N - N_{\mathrm{L}})} \right]^{1/2} \times S_0^2 {b_{xx}}^3 N_{\mathrm{L}} (N - N_{\mathrm{L}})} = 0$$

$$\frac{\partial \sigma_{\mathrm{Tr}}}{\partial N_{\mathrm{L}}} = -\frac{1}{2} \frac{\sigma^2(-2 N_{\mathrm{L}} N + N_{\mathrm{L}}^2 - \exp\{2 b_{xx} \mathrm{Tr}(\mathbf{D})\} N_{\mathrm{L}}^2 + N^2)}{\left[\frac{\sigma^2 (N - N_{\mathrm{L}} + \exp\{2 b_{xx} \mathrm{Tr}(\mathbf{D})\} N_{\mathrm{L}})}{S_0^2 {b_{xx}}^2 N_{\mathrm{L}} (N - N_{\mathrm{L}})} \right]^{1/2} \times S_0^2 {b_{xx}}^2 N_{\mathrm{L}}^2 (N - N_{\mathrm{L}})^2} = 0. \quad [11]$$

Solving these two simultaneous equations gives that the number of measurements with diffusion weighting should be 3.6 times the number without diffusion weighting, and the b factors in the x, y, and z directions should each be $1.28/\mathrm{Tr}(\mathbf{D})$.

Unfortunately, with hardware and physiological limitations on the gradient amplitudes and switching rates, it is not possible to increase the b factor without also increasing the echo time. This necessarily compromises the signal-to-noise in the T_2-weighted images, in the DW images, and in the computed diffusion coefficient images. To further optimize the diffusion weighting, the tissue T_2 and maximum gradient strength available must also be taken into account. For measurement of isotropic diffusion, Chien *et al.* (*4*) showed that there is an optimal TE that gives the smallest measurement error and this value can be estimated by minimizing the random error in the estimated diffusion coefficient, using the standard propagation of errors treatment. Applying the same scheme to the trace of the tensor gives

$$\mathrm{var}(\mathrm{Tr}(\mathbf{D})) = \sigma_{\mathrm{Tr}}^2 = \sigma^2 \left\{ \left[\frac{\partial\ \mathrm{Tr}\{\mathbf{D}\}}{\partial S_1} \right]^2 + \left[\frac{\partial\ \mathrm{Tr}\{\mathbf{D}\}}{\partial S_2} \right]^2 \right\}, \quad [12]$$

where $\mathrm{Tr}\{\mathbf{D}\}$ is calculated as

$$\mathrm{Tr}\{\mathbf{D}\} = -\frac{1}{b} \ln\left(\frac{S_2}{S_1} \right). \quad [13]$$

S_1 is the signal intensity in the image without diffusion weighting, and S_2 is the intensity in the DW image; σ^2 is the variance in signal intensity in the images, which is assumed to be the same in both. Substituting $S_1 = S_0 \exp(-\mathrm{TE}/T_2)$ and $S_2 = S_1 \exp(-b\ \mathrm{Tr}\{\mathbf{D}\})$ gives

$$\sigma_{\mathrm{Tr}}^2 = \left(\frac{\sigma}{S_0} \right)^2 \frac{(1 + \exp(2b\ \mathrm{Tr}\{\mathbf{D}\})) \exp(2\ \mathrm{TE}/T_2)}{b^2}. \quad [14]$$

By minimizing σ_{Tr}^2 with respect to TE, the optimal echo time can be determined.

Eddy Current-Induced Distortions

Haselgrove and Moore (*11*) described the three types of distortion that can occur in echo-planar images due to eddy currents induced by the switching of the diffusion-encoding gradient pulses: translation, produced by a residual gradient in the slice-selection direction and B_0 shift; shear, caused by a residual gradient in the frequency-encoding direction; and scaling, due to a residual gradient in the phase-encoding direction. Eddy currents are induced whenever a gradient is turned on or off and can be considered a superposition of n exponential decay terms (*17*, *18*),

$$J_j(t) = \sum_{i=1}^{n} J_{0i} \exp(-t/\tau_i) \quad (j = 1, \ldots, n), \quad [15]$$

where J_{0i} is constant for the ith contributions (and proportional to the gradient amplitude) and τ_i is the corresponding time constant.

If, for simplicity, we consider just one term, Alexander *et al.* (*19*) showed that the eddy current induced by a pair of gradients of the same duration and strength is given by

$$J(t) = J_0 e^{-t/\tau} [(e^{t_{\mathrm{U1}}/\tau} - e^{t_{\mathrm{D1}}/\tau}) + (e^{t_{\mathrm{U2}}/\tau} - e^{t_{\mathrm{D2}}/\tau})], \quad [16]$$

where t is the time from the start of the sequence, t_{U} and t_{D} are the rise and fall times, and the subscripts 1 and 2 refer to the first and the second pulse.

If the gradient pulses are bipolar, with the same amplitude and duration but with the opposite sign, and $(t_{\mathrm{U1}} - t_{\mathrm{D1}})$ and $(t_{\mathrm{U2}} - t_{\mathrm{D2}})$ are small compared to τ, then the eddy currents from the bipolar pair will tend to cancel each other:

$$J(t) \approx J_0 e^{-t/\tau}[(t_{U1} - t_{D1}) - (t_{U2} - t_{D2})]. \quad [17]$$

In our pulse sequence, detailed below, the gradient waveforms applied in the phase-encoding and readout directions meet this condition; therefore the resulting image magnification and shear are very nearly zero.

Unfortunately, it is not possible to design a simple isotropically weighted sequence with cancellation of eddy currents on all three axes, and with our sequence there is still a residual gradient in the slice-selection direction, which, together with the B_0 shift, produces an image translation in the phase-encode direction. We show later in our experiments that the effect of the residual gradient in the slice-selection direction is small compared to the effect of the B_0 shift. Thus, in the analysis below, we assume that the remaining distortion in the image is an image translation caused by the B_0 shift.

The translation (in mm) in the phase-encode direction can be written as

$$\Delta y = \frac{\gamma \cdot \Delta B_0 \cdot \mathrm{FOV} \cdot \Delta \mathrm{TE}}{2\pi}, \quad [18]$$

where γ is the gyromagnetic ratio; ΔB_0 is the B_0 shift; FOV is the field of view (in mm); and ΔTE is the time between subsequent echoes in the echo-planar sequence. Thus, the shift measured in pixels is expected not to vary with the field of view for a sequence of fixed bandwidth, since $\Delta y \times$ matrix/FOV is the shift measured in pixels.

The B_0 shift that results in translational misalignment between the non-DW and the DW images can be written as

$$\Delta B_0 = G_x k_{B0x} + G_y k_{B0y} + G_z k_{B0z}, \quad [19]$$

where G_x, G_y, and G_z are the components of the applied gradient, **G**, in the three physical directions, and k_{B0x}, k_{B0y}, k_{B0z}, are three constants accounting for the influence of the different gradients on the B_0 shift.

Since the diffusion-weighting gradients are applied in a coordinate system defined by the read, phase-encoding, and slice-selection directions, G_x, G_y, and G_z assume different values according to the orientation of the slice. If we consider the "standard" image orientation to be such that the image lies in the x–y plane, then the image orientation can be specified in terms of two angles α and β which are the rotation angles about the x and y axes, respectively. The logical read and phase-encode directions can be interchanged, although usually with echo-planar imaging, the readout direction will be left–right (for axial or coronal images) or superior–inferior (for sagittal) to avoid peripheral nerve stimulation. For simplicity, then, we assume that we are scanning in the near-axial plane, and that therefore the read direction is left–right (i.e., the scanner x direction when the patient is placed in the scanner head first and supine and performing a pure-axial) and the phase-encoded direction is anterior–posterior (scanner y). Then,

$$\mathbf{G} = \begin{bmatrix} g_{ro}\cos\beta + g_{ss}\sin\beta \\ g_{pe}\cos\alpha + g_{ss}\sin\alpha \\ -g_{ro}\sin\beta - g_{pe}\sin\alpha + g_{ss}\cos\alpha\cos\beta \end{bmatrix}, \quad [20]$$

where g_{ro} is the diffusion-encoding gradient applied in the readout direction, g_{pe} is that applied in the phase-encode direction, and g_{ss} is that applied in the slice-selection direction.

Our sequence allows only single oblique slices; thus we can consider separately a tilt from axial to coronal ($\beta = 0$, arbitrary α) and a tilt from axial to sagittal ($\alpha = 0$, arbitrary β). Then, in the first case, combining Eqs. [18], [19], and [20], the translation is

$$\Delta y(\alpha) = \frac{\gamma \mathrm{FOV} \Delta \mathrm{TE}}{2\pi}[g_{ro}k_{B0x} + (g_{pe}k_{B0y} + g_{ss}k_{B0z})\cos\alpha + (-g_{pe}k_{B0z} + g_{ss}k_{B0y})\sin\alpha], \quad [21]$$

which can be written

$$\Delta y(\alpha) = C_0 + C_1 \sin(\varphi + \alpha), \quad [22]$$

where

$$C_0 = \frac{\gamma \mathrm{FOV} \Delta \mathrm{TE}}{2\pi} g_{ro}k_{B0x}, \quad [23]$$

$$C_1 = \frac{\gamma \mathrm{FOV} \Delta \mathrm{TE}}{2\pi} \times \sqrt{(g_{pe}k_{B0y} + g_{ss}k_{B0z})^2 + (-g_{pe}k_{B0z} + g_{ss}k_{B0y})^2}, \quad [24]$$

and

$$\varphi = \arctan\left[\frac{g_{pe}k_{B0y} + g_{ss}k_{B0z}}{-g_{pe}k_{B0z} + g_{ss}k_{B0y}}\right]. \quad [25]$$

Similarly, in the second case

$$\Delta y(\beta) = D_0 + D_1 \sin(\psi + \beta), \quad [26]$$

where

$$D_0 = \frac{\gamma \mathrm{FOV} \Delta \mathrm{TE}}{2\pi} g_{pe}k_{B0y}, \quad [27]$$

$$D_1 = \frac{\gamma \mathrm{FOV} \Delta \mathrm{TE}}{2\pi} \times \sqrt{(g_{ro}kx + g_{ss}k_{B0z})^2 + (-g_{ro}k_{B0z} + g_{ss}k_{B0x})^2}, \quad [28]$$

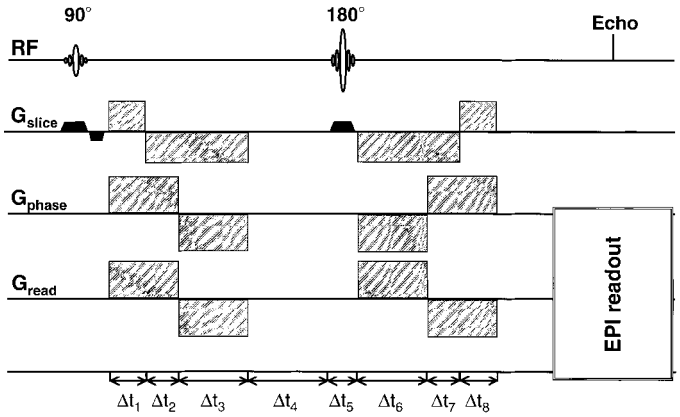

FIG. 1. Pulse sequence for isotropic weighting with low distortion. After the 90° pulse, the diffusion gradients are asymmetrically placed around the refocusing pulse. Gradient durations were as follows: $\Delta t_1 = \Delta t_8 = 10.99$ ms; $\Delta t_1 + \Delta t_2 = \Delta t_3 = \Delta t_6 = \Delta t_7 + \Delta t_8 = 21.41$ ms; $\Delta t_4 = 25.6$ ms; $\Delta t_5 = 7.36$ ms. For other sequence parameters, see the text.

and

$$\psi = \arctan\left[\frac{g_{ro}k_{B0x} + g_{ss}k_{Boz}}{-g_{ro}k_{B0z} + g_{ss}k_{Box}}\right]. \qquad [29]$$

It should therefore be possible to estimate C_0, C_1, D_0, D_1, φ, and ψ from a series of images with different slice orientations, and then use these to correct the translation of the DW images for any subsequent slice orientation.

METHODS

Pulse Sequence

All imaging was performed using a 1.5-T scanner (Siemens Vision, Erlangen, Germany), using the spin-echo echo-planar pulse sequence shown in Fig. 1. Fat suppression was performed using a four RF pulse binomial pulse train to avoid the chemical shift artifact. For each slice, one T_2-weighted image was collected and then three DW images, each using identical diffusion-encoding waveforms. A birdcage head coil of ~300 mm diameter was used for both RF transmission and for reception of the signal. The maximum gradient strength available was 24 mT m^{-1} along each of the physical gradient axes. However, because of the long duration of the diffusion-encoding pulses, and the need for the pulse sequence to allow single-oblique slices to be prescribed, an amplitude of 17 mT m^{-1} was used for the diffusion-encoding pulses in the read and phase-encode directions, and 13.26 mT m^{-1} in the slice-selection direction for this pulse sequence.

Optimization of the gradient b factor and echo time from consideration of Eq. [12] led to a TE of 160 ms and a b factor of 289 s mm^{-2} being used in each of the read, phase-encode, and slice-selection directions. The shape of the pulses and their durations are shown in Fig. 1.

The EPI readout consisted of 128 lines, with receiver bandwidth of 160 kHz, with a time between subsequent lines of 800 μs. A constant phase-encoding gradient was used with continuous sampling of the NMR signal (128 points per line) and sinusoidal ramp up and down of the read gradient. The manufacturer's own phase correction and regridding algorithm were used before Fourier transformation and interpolation to a 256 × 256 image matrix. Sixteen slices were collected with a field of view of 240 mm, and a slice thickness of 5 mm with a 1-mm gap between slices. Slices were acquired in ascending order such that positionally adjacent slices were acquired sequentially. A scan repetition time (i.e., the time between the first T_2-weighted slice and the first and subsequent DW slices) of 9 s was used, with all 16 slices acquired as quickly as possible (in about 3.5 s), thus leaving about 5.5 s delay before repeated acquisition of the slice block in order to allow long time constant eddy currents to die away.

Measurement of Eddy Current-Induced Distortions

In order to verify Eqs. [22] and [26] and to estimate the constants (C_0, C_1, φ, D_0, D_1, and ψ) we imaged a polymer gel phantom (*20*). Gel was chosen for the phantom material because of its moderate T_2 and low diffusion coefficient so that the intensities of the T_2-weighted and DW images were similar. In addition, the gel phantom was insensitive to the vibrations caused by the diffusion-encoding gradients that can cause surface waves in liquid phantoms. An internal structure was formed within the gel by irradiating it using a 6-MeV X-ray source. Three 4 × 4-cm orthogonal radiation fields were applied, giving a total dose of 10 Gy in the overlap.

The image data were transferred to an independent workstation (Sun Sparcstation, Sun Microsystems, Mountain View, CA) for postprocessing. First, an average DW image for each slice position was formed from the three separate DW images. Then, the distortion of the average DW image was assessed using a method similar to that used by Haselgrove and Moore (*10*), but the similarity between the T_2-weighted and DW images was measured by evaluating the mutual information carried by the two images (*21*):

$$I(M, N) = \sum_{m\in M}\sum_{n\in N} p\{m, n\}\log\frac{p\{m, n\}}{p\{m\}p\{n\}}, \qquad [30]$$

M and N are the sets of all the intensity values present in the T_2-weighted image and in the DW image, respectively; $p\{m\}$ and $p\{n\}$ are the probability of occurrence of individual intensities on each image and $p\{m, n\}$ is the joint probability of occurrence of the pair m–n. Maximizing the mutual information by varying the shift, shear, and scale using the downhill simplex method (*22*) allowed the distortion to be measured. The distortion was measured separately for each of the 16 slices.

Measurements were made from the phantom with single-oblique slice tilts from axial to coronal in steps of 15°, and then from axial to sagittal again in steps of 15°. Sixteen slices were acquired at each rotation angle. From plots of translation vs image plane rotation angle the parameters in Eqs. [22] and [26] describing the image distortion were estimated.

Correction of Patient Data

Having found the image distortion as a function of the image plane rotation angles, these were then used to correct images collected in a clinical setting, according to Eqs. [22] and [26]. The average of the three DW images was calculated to improve the signal-to-noise ratio, and then the distortion correction was performed. Finally, an image of the mean diffusivity (=Tr(**D**)/3) was produced by performing the following calculation on a pixel-by-pixel basis:

$$\text{mean diffusivity} = -\frac{1}{3b}\ln\left(\frac{S_{av}}{S_1}\right). \qquad [31]$$

b is the b factor along any one axis, and the three b factors are all equal; S_{av} is the average DW signal intensity; and S_1 is the T_2-weighted signal intensity ($b \approx 0$).

RESULTS

Eddy Current-Induced Distortions

Figure 2 shows one plot of estimated magnification, shear, and translation for a pure axial DW image of the phantom. The isotropically weighted sequence is compared with a standard manufacturer's diffusion-weighted sequence with the same bandwidth, which collects three diffusion-weighted images per slice, each weighted along one axis. It can be seen that with the standard sequence the distortions are greater and, furthermore, applying the diffusion gradients on the three axes separately leads to different values of shift, shear, and scale on each image, making the correction difficult to perform. With the isotropically weighted sequence the magnification (Fig. 2a) is approximately unity while the shear (Fig. 2b) is slightly worse than expected (approximately 0.005). This is probably due to the fact that, although the shear is caused by a residual gradient in the readout direction and the gradients are compensated along this axis, gradient pulses in orthogonal directions can also cause residual gradients in the readout direction. The image translation (Fig. 2c) changes over the first few slices of this image, before it settles down to an almost constant value. In the subsequent plots below, the image translations are estimated from the average of the last 12 slices out of 16, and so represent the distortions that occur in the steady state.

In order to show that the translation is independent of the slice position, we compared the sets of 16 slices acquired in a pure axial plane with ascending and descending slice excitation order. In Fig. 3, the estimated distortion is plotted vs the excitation order: the translation is approximately the same for both measurements, even though the slice position is reversed.

Figure 4 shows the estimated average image translation in the DW image for rotations of the image plane away from true axial toward coronal (Fig. 4a) and toward sagittal (Fig. 4b). In all cases the translation follows the sinusoidal pattern predicted by Eqs. [22] and [26]. From the data presented in Fig. 4, the distortion parameters were estimated by nonlinear least-squares fitting, and are shown in Table 1.

Image Correction

Figure 5 shows the result of applying the estimated image translation correction to data collected from a patient who had suffered an acute stroke. The images were acquired with a 260-mm FOV, but with acquisition parameters otherwise identical to those given above. As shown before, the translation measured in pixels is independent of the FOV. Figures 5a and 5b show the T_2-weighted and one of the three DW images respectively, while Fig. 5c shows the average of the three DW images. Figure 5d shows a calculated mean diffusivity image produced without correction for translation of the DW image (image 5c), and Fig. 5e shows the mean diffusivity calculated after correction. Note the artifacts in Fig. 5d resulting from misregistration of the T_2-weighted and DW images, shown in detail in Fig. 5f.

DISCUSSION

We have shown that a particular design of an echo-planar pulse sequence that gives diffusion weighting only dependent on the trace of the diffusion tensor also has inherently low image distortion due to gradient-induced eddy currents. We have also shown the theoretical optimal number of images and diffusion weighting factors that should be used with this image acquisition scheme if it is to be used for estimation of the diffusion tensor trace. This involves collecting approximately three DW images for every one T_2-weighted image.

Because of the relatively simple image distortions that occur, they can be corrected relatively straightforwardly by first characterizing the distortion using phantom scans, and then using these characteristics in a postprocessing scheme. The distortions should not change unless modifications to the imaging gradient hardware are made, in which case the required remeasurement is fairly quick to perform.

The simplicity of the image distortion is ensured if three criteria are met. First, by using a relatively long delay between successive multislice acquisitions, the image distortions in the first set of DW images are the same as those in the subsequent sets of DW images. The minimum delay needed for the long time constant eddy currents to die away between successive slice blocks was found experimentally to be about 5 s for our scanner. Thus, DW images can simply be averaged to improve

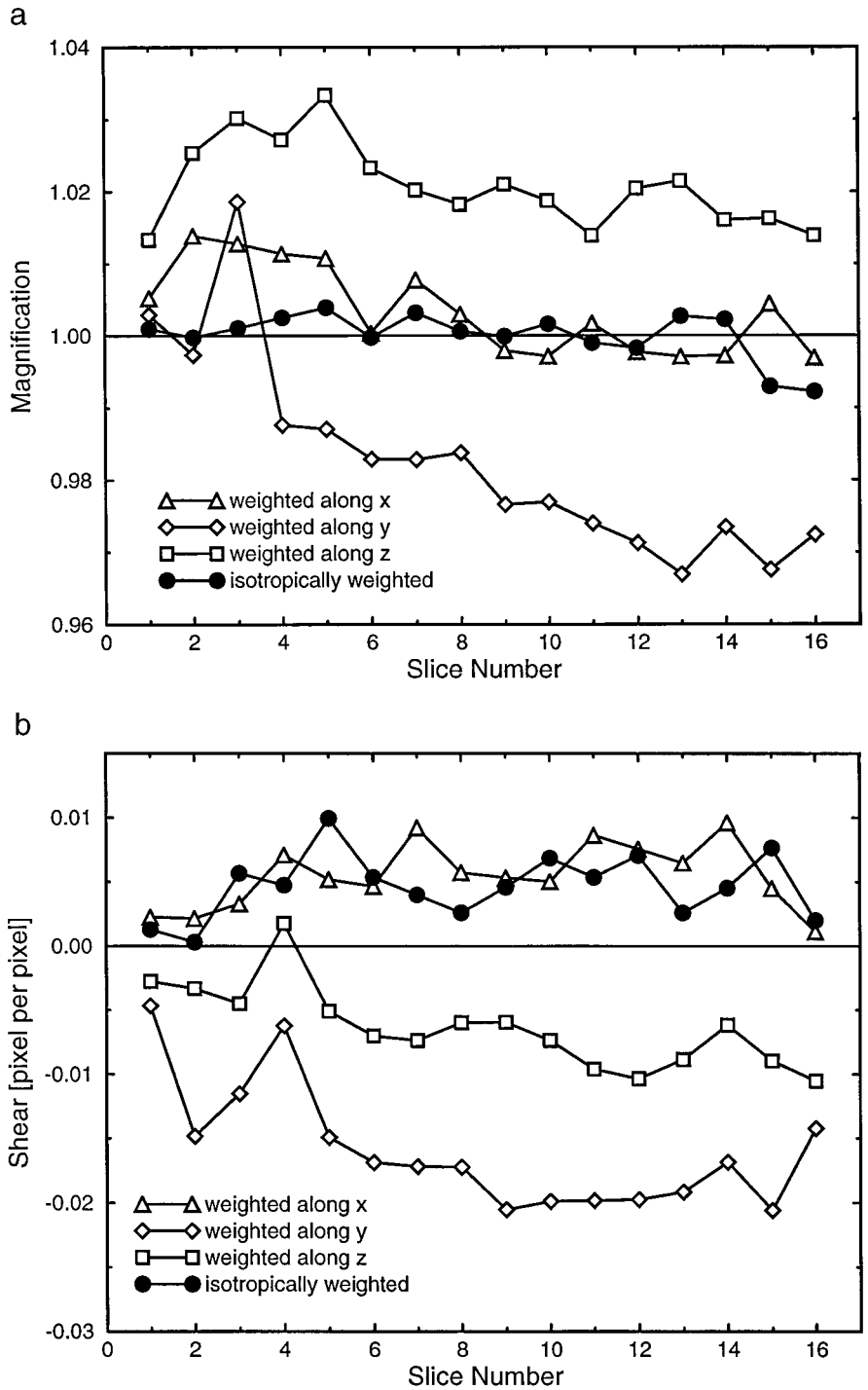

FIG. 2. Estimated distortion vs slice number for a pure axial scan. The isotropically weighted sequence is compared to a standard sequence with weighting applied separately on the three axes. (a) Magnification; (b) shear; and (c) translation.

the signal-to-noise ratio without different corrections being needed for each one.

Second, the first few slices of a DW multislice data set show different distortions because of medium-term time constant eddy currents. This is not a problem if a few extra slices than are actually required for anatomical coverage are acquired, and then discarded or ignored. The remaining slices will then all have virtually identical image distortion.

Third, diffusion-encoding gradient pulses in the read and phase-encoded directions consist of pairs of bipolar pulses, and the eddy currents generated from these tend to be self-compensating. We chose to apply these self-compensating pulses in

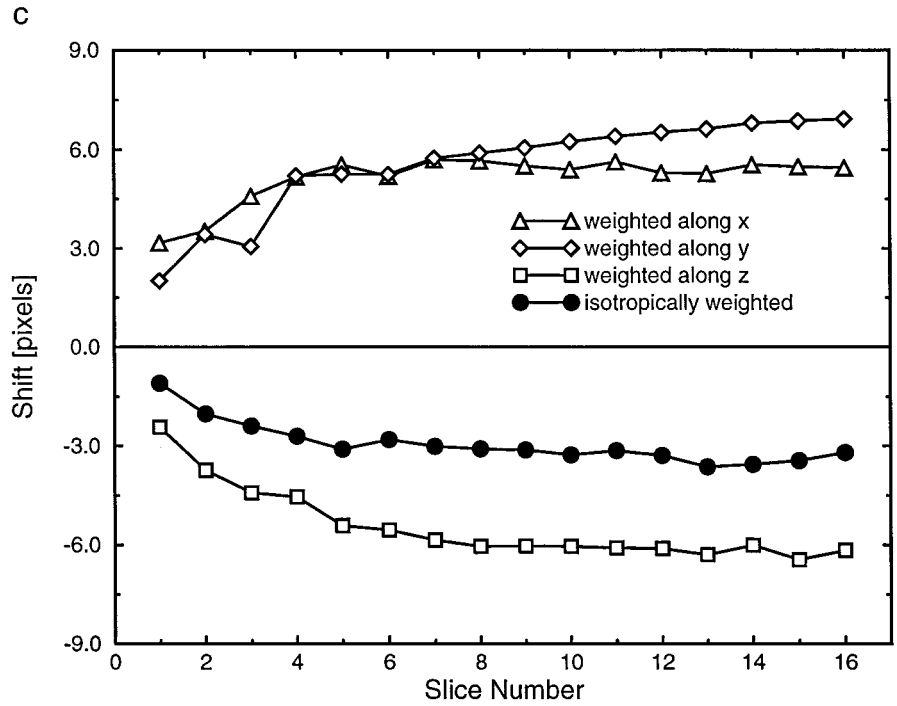

FIG. 2—*Continued*

the read and phase directions, rather than the slice-selection direction, because it then becomes an easy matter to satisfy the condition that the off-diagonal elements of the **b** matrix are all zero. Because a slice-selection gradient pulse must be positioned halfway through a spin-echo sequence, it is easiest to ensure a null interaction between the diffusion weighting pulses in the read and phase-encoding directions by making the **k** vector zero for these directions at the time of the refocusing

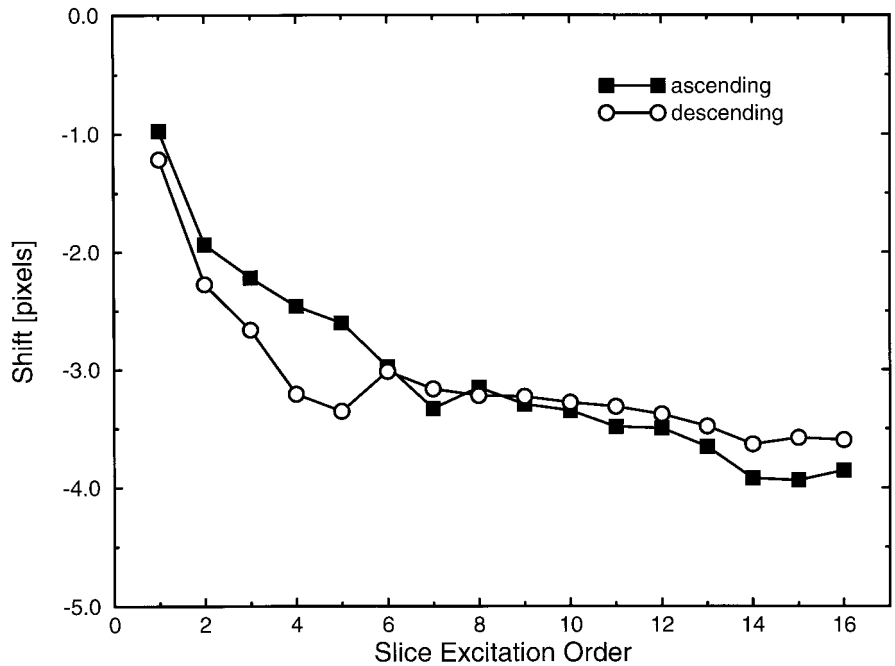

FIG. 3. Estimated translation vs slice excitation number for a pure axial scan. Images collected with ascending excitation order are compared to images collected with descending excitation order, to show that distortion is independent of slice position.

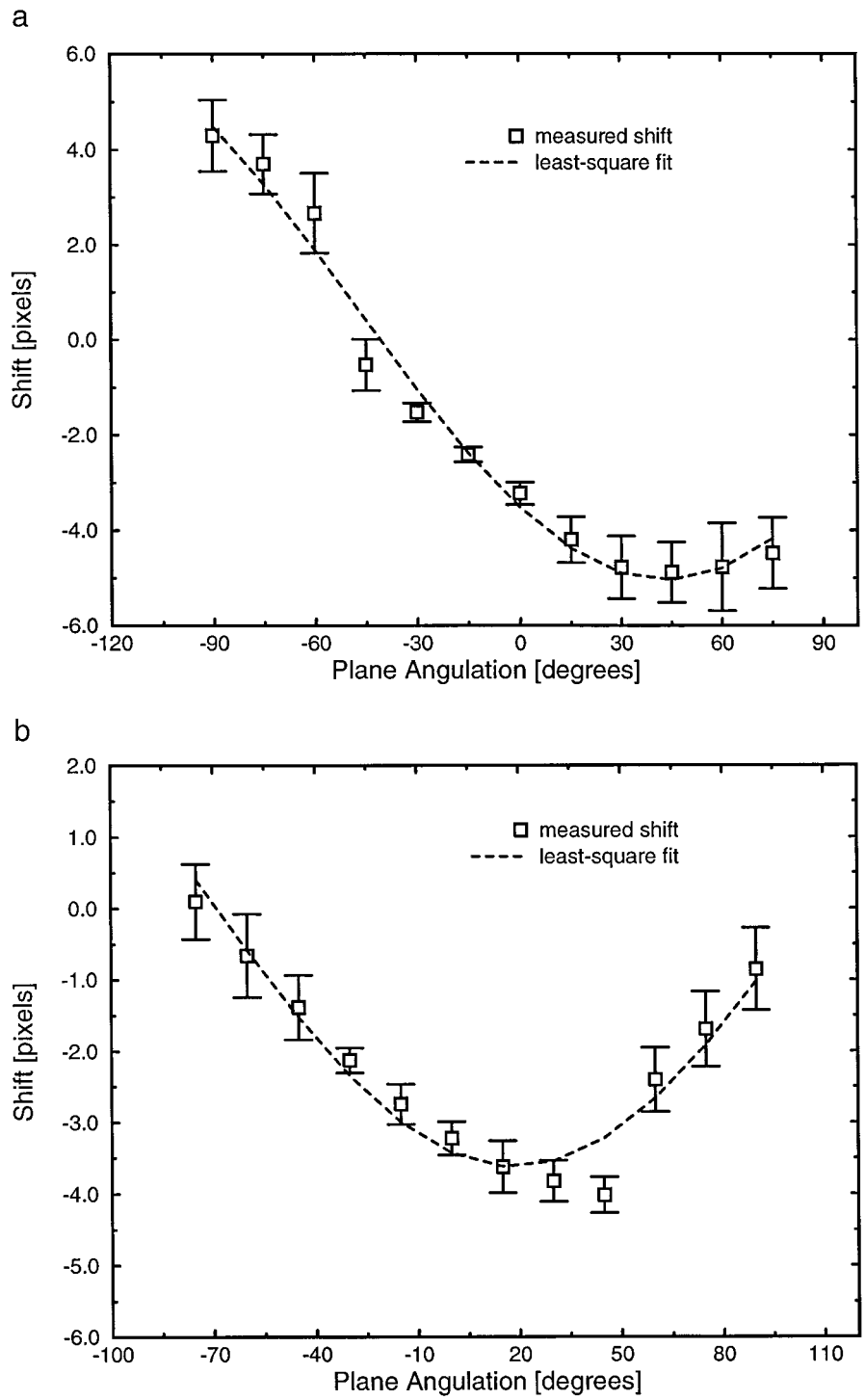

FIG. 4. Average translation vs image plane orientation for off-axial scans: axial toward coronal (a) and axial toward sagittal (b). The data are fitted with the curves obtained substituting the values reported in Table 1 into Eqs. [23] and [27], respectively.

pulse. While it is possible that gradient pulses in one direction can result in eddy current-induced gradients in another direction (*23*), our data, showing that the image shear and scale are small, suggest that these terms are negligible for this sequence. Our correction scheme could potentially incorporate correction of all the three parameters (scale, shift, and shear) at the same time.

Figure 2 shows that for true axial slices, the image translation settles down to a constant value after a few slices have been acquired and that therefore in a steady state, the image

TABLE 1
Image Translation Parameters in Eqs. [23]–[39], Estimated by Nonlinear Least-Squares Fitting

C_0	0.638
C_1	−5.68
φ	47.2°
D_0	0.185
D_1	−3.81
ψ	71.6°

translation is independent of the slice position. This was true regardless of the slice position, as shown in Fig. 3. Thus we can confirm, at least for our scanner, that the translation is due mainly to a uniform B_0 shift.

Of course, a better signal-to-noise ratio could be achieved by giving diffusion weighting separately in the read, phase, and slice directions in the three DW images, since the same diffusion weighting could have been achieved at a shorter echo time. However, the three DW images would have suffered different image distortions, making their combination problematical. Use of bipolar gradient schemes to try to reduce the image distortion (*19*) would have resulted in even longer echo times than for the isotropically weighted sequence presented here.

The small and relatively simple image distortion for our sequence allows the distortion to be characterized by a set of straightforward measurements on a phantom; this can then be used to correct any oblique slice orientation. Alternatively, the eddy current-induced field shifts can be measured at the time the sequence is run (*23, 24*) and used to correct the *k*-space data. This has the advantage that if the eddy current characteristics of the scanner change over time then the distortion correction will still perform well. However, this must be offset against the increased imaging time needed during scanning, and the fact that the patient data will have an inherently poorer

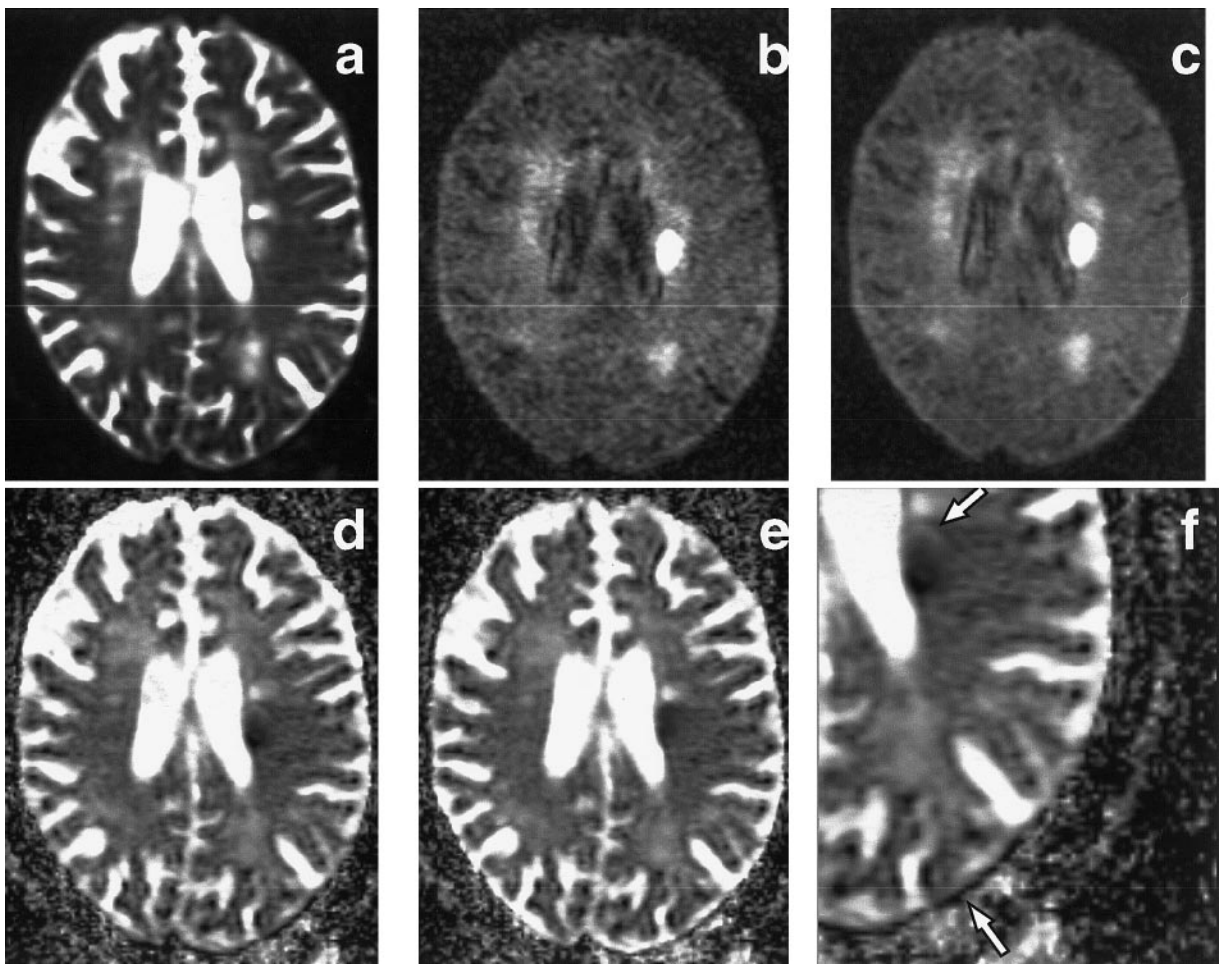

FIG. 5. Images of a patient who suffered an acute stroke: T_2-weighted (a) and diffusion-weighted (b). The phase-encoding direction is vertical. It can be seen how noise is reduced in the average (c) of the three diffusion-weighted images, compared with (b). The stroke is clearly visible in both the computed mean diffusivity images, before correction (d) and after correction (e), but the distortion in the uncorrected image shows up as edge artifacts, as pointed to by the arrow in (f). Artifacts appear also where CSF is present, as indicated.

signal-to-noise ratio than measurements made from a phantom. In principle, an arbitrarily high signal-to-noise ratio in the phantom data can be achieved by signal averaging, leading to excellent characterization of the image distortion. Finally, patient motion during the acquisition of reference phase data for correction can lead to inaccurate corrections.

CONCLUSIONS

We have shown that a design of a pulse sequence that gives diffusion weighting dependent on the trace of the diffusion tensor also results in small, easily characterizable eddy current-induced distortions that can be corrected by postprocessing. The echo time and gradient *b* factors have been optimized to give the maximum signal-to-noise ratio in the computed mean diffusivity image, and this sequence is now in routine clinical use.

ACKNOWLEDGMENTS

M. Cercignani is thankful to the Neuroimaging Research Unit, Department of Neurology, Scientific Institute Ospedale San Raffaele, University of Milan, for financial support. Both the authors also express their thanks to the Glenfield Hospital N.H.S. trust for allowing access to the MRI scanner on which this study was performed.

REFERENCES

1. S. Warach, J. F. Dashe, and R. R. Edelman, Clinical outcome in ischemic stroke predicted by early diffusion-weighted and perfusion magnetic resonance imaging: A preliminary analysis, *J. Cereb. Blood Flow Metab.* **16,** 53–59 (1996).
2. A. de Crespigny, M. P. Marks, D. R. Enzmann, and M. E. Moseley, Navigated diffusion imaging of normal and ischemic human brain, *Magn. Reson. Med.* **33,** 720–728 (1995).
3. S. Warach, D. Chien, W. Li, M. Ronthal, and R. Edelman, Fast magnetic resonance diffusion-weighted imaging of acute human stroke, *Neurology* **42,** 1717–1723 (1992).
4. D. Chien, R. Buxton, K. Kwong, T. Brady, and B. Rosen, MR diffusion imaging of the human brain, *J. Comput. Assist. Tomogr.* **14,** 514–520 (1990).
5. K. Butts, J. Pauly, A. J. de Crespigny, and M. E. Moseley, Isotropic diffusion-weighted and spiral-navigated interleaved EPI for routine imaging of acute stroke, *Magn. Reson. Med.* **38,** 741–749 (1997).
6. M. Eis, T. Els, M. Hoehn-Berlage, and K. A. Hossmann, Quantitative diffusion MR imaging of cerebral tumor and edema, *Acta Neurochir. Suppl.* **60,** 344–346 (1994).
7. P. Christiansen, P. Gideon, C. Thomsen, M. Stubgaard, O. Henriksen, and H. B. W. Larsson, Increased water self-diffusion in chronic plaques and in apparently normal white matter in patients with multiple sclerosis, *Acta Neurol. Scand.* **87,** 195–199 (1993).
8. M. A. Horsfield, M. Lai, S. L. Webb, G. J. Barker, P. S. Tofts, R. Turner, P. Rudge, and D. H. Miller, Apparent diffusion coefficients in benign and secondary progressive multiple sclerosis by nuclear magnetic resonance, *Magn. Reson. Med.* **36,** 393–400 (1996).
9. A. W. Anderson and J. C. Gore, Analysis and correction of motion artifacts in diffusion weighted imaging, *Magn. Reson. Med.* **32,** 379–387 (1994).
10. R. Turner, D. LeBihan, J. Maier, R. Vavrek, L. K. Hedges, and J. Pekar, Echo-planar imaging of intravoxel incoherent motion, *Radiology* **177,** 407–414 (1990).
11. J. C. Haselgrove and J. R. Moore, Correction for distortion of echo-planar images used to calculate the apparent diffusion coefficient, *Magn. Reson. Med.* **36,** 960–964 (1996).
12. P. J. Basser, J. Mattiello, and D. LeBihan, MR diffusion tensor spectroscopy and imaging, *Biophys. J.* **66,** 259–267 (1994).
13. P. van Gelderen, M. H. de Vleeschouwer, D. DesPres, J. Pekar, P. C. van Zijl, and C. T. Moonen, Water diffusion and acute stroke, *Magn. Reson. Med.* **31,** 154–163 (1994).
14. E. C. Wong, R. W. Cox, and A. W. Song, Optimized isotropic diffusion weighting, *Magn. Reson. Med.* **34,** 139–143 (1995).
15. T. Chun, A. M. Ulug, and P. C. M. van Zijl, Single-shot diffusion-weighted trace imaging on a clinical scanner, *Magn. Reson. Med.* **40,** 622–628 (1998).
16. Y. Bito, S. Hirata, and E. Yamamoto, Optimal gradient factors for ADC measurements, *in* "Proceedings, ISMRM, 3rd Scientific Meeting, Nice," p. 913 (1995).
17. C. B. Ahn and Z. H. Cho, Analysis of eddy currents in nuclear magnetic resonance imaging, *Magn. Reson. Med.* **17,** 149–163 (1991).
18. B. R. Barker, B. T. Archer, W. A. Erdman, and R. M. Peshock, A MRI gradient waveform model for automated sequence calibration, *Med. Phys.* **19,** 1483–1489 (1992).
19. A. L. Alexander, J. S. Tsuruda, and D. L. Parker, Elimination of eddy current artifacts in diffusion-weighted echo-planar images: The use of bipolar gradients, *Magn. Reson. Med.* **38,** 1016–1021 (1997).
20. M. J. Maryanski, R. J. Schulz, G. S. Ibbott, J. C. Gatenby, J. Xie, D. Horton, and J. C. Gore, Magnetic resonance imaging of radiation dose distributions using a polymer-gel dosimeter, *Phys. Med. Biol.* **39,** 1437–1455 (1994).
21. C. Studholme, D. L. G. Hill, and D. J. Hawkes, Automated three-dimensional registration of magnetic resonance and positron emission tomography brain images by multiresolution optimization of voxel similarity measures, *Med. Phys.* **24,** 25–35 (1996).
22. A. J. de Crespigny and M. E. Moseley, Eddy current induced image warping in diffusion weighted EPI, *in* "Proceedings, ISMRM, 6th Scientific Meeting, Sidney," p. 661 (1998).
23. P. Jezzard, A. S. Barnett, and C. Pierpaoli, Characterization of and correction for eddy current artifacts in echo-planar diffusion imaging, *Magn. Reson. Med.* **39,** 801–812 (1998).
24. F. Calamante, D. A. Porter, D. G. Gadian, and A. Connelly, Correction for eddy current induced B_0 shifts in diffusion weighted EPI, *in* "Proceedings, ISMRM, 6th Scientific Meeting, Sidney," p. 662 (1998).